Climbing-fibre activation of NMDA receptors in Purkinje cells of adult mice

Massimiliano Renzi, Mark Farrant and Stuart G. Cull-Candy

Department of Pharmacology, University College London, Gower Street, London WC1E 6BT, UK

Among principal neurons, adult Purkinje cells have long been considered unusual in lacking functional NMDA receptors. This view has emerged largely from studies on rats, where NMDA receptors are expressed in Purkinje cells of newborn animals, but are lost after 2 weeks. By contrast, immunolabelling data have shown that Purkinje cells from adult mice express multiple NMDA receptor subunits, suggesting a possible species difference. To investigate the presence of functional NMDA receptors in Purkinje cells of mice, and to explore the contribution of different receptor subunits, we made whole-cell and single-channel patch-clamp recordings from Purkinje cells of wild-type and NR2D−/− mice of different ages. Here we report that multiple NMDA receptor subtypes are indeed expressed in Purkinje cells of young and adult mice; in the adult, both NR2A- and NR2B-containing subtypes are present. Furthermore, we show that NMDA receptor-mediated EPSCs can be evoked by climbing fibre stimulation, and appear to be mediated mainly by NR2A-containing receptors.

(Resubmitted 26 July 2007; accepted after revision 26 September 2007; first published online 27 September 2007)
Corresponding author S. Cull-Candy: Department of Pharmacology, University College London, Gower Street, London WC1E 6BT, UK. Email: s.cull-candy@ucl.ac.uk

N-Methyl-D-aspartate receptors (NMDARs) are widely expressed in the central nervous system, playing key roles in synaptic transmission, synaptic plasticity and synaptogenesis (Dingledine *et al.* 1999; Cull-Candy *et al.* 2001; van Zundert *et al.* 2004). Three main families of NMDAR subunits have been identified, namely NR1, NR2 and NR3 (see Cull-Candy *et al.* 2001; Neyton & Paoletti, 2006). Most native NMDARs are heteromeric assemblies formed from a dimer of NR1 subunits together with a dimer of NR2 subunits (Furukawa *et al.* 2005). The functional and pharmacological properties of NMDARs depend critically on the identity of their NR2 subunits. The NR2 family consists of four members (NR2A, -2B, -2C and -2D) which show striking regional variation, with specific NR2 subunits being restricted to defined neuronal populations. Furthermore, NR2 subunit expression changes during development, and is influenced by activity (Cull-Candy *et al.* 2001; van Zundert *et al.* 2004).

Purkinje cells (PCs) are thought to express NMDARs only transiently and only in the extrasynaptic membrane. Thus, low-conductance NR2D-containing NMDAR channels are present in PCs from young rats (Momiyama *et al.* 1996). However, these are not activated during synaptic transmission, even during climbing fibre (CF) activity (Momiyama *et al.* 2003). Furthermore, these receptors are lost after postnatal day (P)12 (Momiyama *et al.* 1996). Accordingly, in juvenile and adult rats, CF stimulation gives rise to currents that are mediated predominantly by α-amino-3-hydroxy-5-methyl-4-isoxazolepropionic acid receptors (AMPARs), with contributions from kainate receptors, metabotropic glutamate receptors and glutamate transporters (Otis *et al.* 1997; Auger & Attwell, 2000; Dzubay & Otis, 2002; Huang *et al.* 2004) but not from NMDARs (Perkel *et al.* 1990; Farrant & Cull-Candy, 1991; Llano *et al.* 1991; Otis *et al.* 1997; Auger & Attwell, 2000). Surprisingly, however, adult PCs are known to be susceptible to a variety of pathological conditions thought to involve excitotoxicity normally associated, in other neurons, with the presence of NMDARs (Slemmer *et al.* 2005). Furthermore, rat PCs contain the NR1 protein within intracellular organelles (Petralia *et al.* 1994), and this is able to form functional NMDARs when the cells are infected with recombinant virus encoding the NR2B subunit (Kakegawa *et al.* 2003).

In the present study, we initially investigated the expression and subunit composition of NMDARs in PCs from young mice. To this end, we examined whether PCs from NR2D knockout (NR2D−/−) mice (Ikeda *et al.* 1995) lacked the low-conductance form of NMDAR. While these were indeed absent, high-conductance NMDAR channels were found in patches from both wild-type and NR2D−/− mice, indicating the presence of other NMDAR subtypes in young PCs. This raised the possibility that functional high-conductance NMDARs may also be expressed in PCs from adult mice, as suggested by

 DOI: 10.1113/jphysiol.2007.141531

immunolabelling data (Thompson *et al.* 2000). Our experiments show that NMDARs are present in the adult (~80% of PCs tested), and that NMDAR-mediated EPSCs can be evoked by CF stimulation (~50% of PCs tested). Interestingly, adult human tissue shows labelling for NR1, NR2A and NR2D mRNA in PCs (Scherzer *et al.* 1997), and the expression of functional NMDARs in PCs, as shown here, may therefore help explain why human PCs are susceptible to a variety of pathological conditions thought to involve excitotoxicity (Slemmer *et al.* 2005).

Methods

Cerebellar slices

Male and female C57BL/6 and NR2D−/− mice, aged between postnatal days 5 and 84 (P5–84), were anaesthetized with isoflurane and decapitated in accordance with the UK Animals (Scientific Procedures) Act 1986. The brains were removed and dissected in cold (0.5–4°C) oxygenated 'slicing' solution, containing (mM): 85 NaCl, 2.5 KCl, 0.5 $CaCl_2$, 4 $MgCl_2$, 25 $NaHCO_3$, 1.25 NaH_2PO_4, 75 sucrose, 25 glucose, 0.01 D-(−)2-amino-5-phosphonopentanoic acid (D-AP5); pH 7.4, when bubbled with 95% O_2 and 5% CO_2. Parasagittal slices (250–300 μm) were cut from the cerebellar vermis (HM 650V; Microm International GmbH, Walldorf, Germany). Slices were incubated at 32°C for 40 min and thereafter at room temperature, during which time the sucrose containing slicing solution was gradually replaced by a standard 'external' solution containing (mM): 125 NaCl, 2.5 KCl, 2 $CaCl_2$, 1 $MgCl_2$, 25 $NaHCO_3$, 1.25 NaH_2PO_4 and 25 glucose; pH 7.4, when bubbled with 95% O_2 and 5% CO_2.

Slices were transferred to a submerged recording chamber and perfused with oxygenated external solution (1.5–2.5 ml min^{-1}). Neurons were visualized under infrared differential interference contrast optics (Zeiss Axioskop; Zeiss, Oberkochen, Germany). Patch-clamp recordings were made at room temperature (25 ± 1°C) with an Axopatch-200A amplifier (Molecular Devices Corp., Sunnyvale, CA, USA).

Solutions

Whole-cell. The standard 'external' solution was as above, except that $MgCl_2$ was omitted. All experiments were made in the presence of 1 μM strychnine hydrochloride and 10 μM 6-imino-3-(4-methoxyphenyl)-1(6*H*)-pyridazinebutanoic acid hydrobromide (SR-95531). NMDA-activated currents were recorded in response to 50 or 100 μM *N*-methyl-D-aspartate (NMDA) in the presence of 50 μM glycine, 1 μM tetrodotoxin and 10 μM 2,3-dioxo-6-nitro-1,2,3,4-tetrahydrobenzo[f]quinoxaline-7-sulphonamide (NBQX). In experiments investigating the NMDAR-mediated component of CF-EPSCs, strychnine was increased to 5 μM, SR-95531 to 40 μM and glycine to 200 μM, NBQX was used at 1 and 20 μM, and metabotropic glutamate receptors (GluR1α) were blocked with 100 μM (*S*)-(+)-α-amino-4-carboxy-2-methylbenzeneacetic acid (LY367385).

Outside-out patches. The nominally Mg^{2+}-free 'external' solution was as above except that $CaCl_2$ was reduced to 1 mM. All experiments were made in the presence of 1 μM strychnine, 10 μM SR-95531 and 5 μM 6-cyano-7-dinitroquinoxalinedione (CNQX). In experiments on adult mice, 1 μM tetrodotoxin was added to the solution. NMDA-activated currents were recorded in response to 10 μM NMDA and in the presence of 5 μM glycine in patches from PCs from young mice, or in response to 50 or 100 μM NMDA and in the presence of 50 μM glycine in patches from PCs from adult mice. In experiments investigating the sensitivity of NMDARs to external Zn^{2+} ions, the recording solution contained 10 mM tricine, in order to buffer Zn^{2+} in the nanomolar range (Paoletti *et al.* 1997). Only one patch was excised from each PC tested.

The 'intracellular' (pipette) solution, used for both whole-cell and outside-out recordings, contained (mM): 140 CsCl; 4 NaCl; 0.5 $CaCl_2$; 10 *N*-2-hydroxyethylpiperazine-*N*′-2-ethanesulphonic acid (Hepes); 5 ethyleneglycol-bis (β-aminoethylether)-*N*,*N*,*N*′,*N*′-tetraacetic acid (EGTA); 2 Mg-ATP (adjusted to pH 7.3 with CsOH). In some experiments on PCs from adult mice, we used a pipette solution containing 30 mM 1,2-bis(o-aminophenoxy)ethane-*N*,*N*,*N*′,*N*′-tetraacetic acid (BAPTA, CF-EPSC recordings) and/or 1 mM *N*-(2,6-imethylphenylcarbamoylmethyl) triethylammonium chloride (QX314 chloride, CF-EPSC recordings and single-channel recordings).

All drugs were obtained from Tocris Bioscience (Bristol, UK), apart from strychnine (Sigma, Poole, UK) and glycine (BDH, Poole, UK).

Recording procedures

For whole-cell recording, pipettes were made from thin-walled borosilicate glass tubing (1.5 mm o.d., 1.17 mm i.d.; G150TF-3; Warner Instruments LLC, Hamden, CT, USA). For patch recording, pipettes were pulled either from the same glass or from thick-walled borosilicate glass tubing (1.5 mm o.d., 0.86 mm i.d.; GC-150F; Harvard Apparatus Ltd, Edenbridge, UK). Pipettes were coated with Sylgard resin (Dow Corning 184) and fire polished just prior to use to a final resistance of 2–15 MΩ (single-channel recordings, see text) or 2–6 MΩ (whole-cell recordings). Single-channel activity was studied at least 30 s after the application of drugs (steady-state conditions).

Paired CF-EPSCs were evoked by stimuli delivered with a glass pipette (containing external solution) positioned within the granule cell layer and ∼50–100 μm from the PC (stimulation: 70–100 V, 20–40 μs duration at 0.033 Hz, paired pulse interval 500 ms; Digitimer DS2 isolated stimulator, Digitimer Ltd, Welwyn Garden City, UK). After CF-EPSC detection, the stimulus strength was set 20 V above the threshold and the peak current was monitored. Stable CF-EPSCs were recorded for ∼5 min before drug application. Whole-cell and synaptic currents were recorded after 60–70% series resistance compensation (typically 7 μs lag time). PCs showing a $>$ 20% increase of the series resistance were discarded. Data were stored on digital audio-tape (BioLogic DTR-1204; DC to 20 kHz) for later analysis.

Data analysis

Data were replayed from tape, and filtered at 2 kHz (single-channel and CF-EPSC data) or 1 kHz (whole-cell current data) using a low pass 8th order Bessel external filter and digitized at 10 or 5 kHz, respectively (Digidata 1200, pCLAMP 8, Molecular Devices). Single-channel data were fitted with the step-response function of the recording system using the time course fitting method (SCAN) and data were analysed and displayed using the program EKDIST (http://www.ucl.ac.uk/Pharmacology/dc.html). Any events briefer than two filter rise times (i.e. $<$ 98.8% of their full amplitude) were excluded from the analysis of fitted amplitudes. To estimate the channel slope conductance, current amplitude histograms were constructed from un-binned data and fitted to the sum of two or three Gaussian components, using the maximum likelihood method. The mean amplitudes obtained were then plotted against voltage, and the data were fitted by linear regression. Where appropriate, a correction for a calculated liquid junction potential of 5.3 mV was applied. For the 'asymmetry plot' (Fig. 1*D*), the occurrence of transitions between two open states (represented as the i^{th} conductance level followed by the $(i+1)^{\text{th}}$ conductance level, where i is an integer) was estimated and shown as a 3D-distribution of the frequency of the various transition types. Charge transfer analysis of single-channel currents was performed on consecutive 10 s epochs using Fetchan (pCLAMP 8; Molecular Devices). At least 12 epochs ($\geq$ 2 min of recording) were analysed in the presence of NMDA (before the application of Zn^{2+} or ifenprodil). To control for possible slow changes in channel activity, a line was fitted through a plot of charge against elapsed time (IGOR Pro 5.0; Wavemetrics, Lake Oswego, OR, USA). The effect of Zn^{2+} or ifenprodil was then estimated as the ratio between the average of the charge transfer measured in the presence of the test treatment and the average of the corresponding values from the extrapolated linear fit to the control values.

Measurements of CF-EPSCs (peak, area, 10–90% rise time and 37% decay) were taken from averaged waveforms generated from 5 to 18 consecutive events (IGOR Pro and NeuroMatic, http://www.neuromatic.thinkrandom.com).

Statistical analysis

All values are expressed as means ± S.E.M. Differences between groups were tested using a paired Student's t test (unless stated otherwise). Where data were not normally distributed (Shapiro–Wilk test) they were compared using a Wilcoxon matched pairs test (Prism 3.0, GraphPad Software Inc., San Diego, CA, USA).

Results

Low- and high-conductance NMDAR channels in young PCs

In our experiments on young mice (P5–9), we found that application of NMDA activated low-conductance single-channel currents (∼40 and 20 pS) in all PC patches examined (Fig. 1). As expected from our previous experiments on rat PCs in slices (Momiyama *et al.* 1996), the properties of these events were consistent with those of NR2D-containing NMDARs (Fig. 1*B–D*, see legend for details; Wyllie *et al.* 1996; Cull-Candy *et al.* 2001). Furthermore, we found that NR2D−/− animals (Ikeda *et al.* 1995), lacked the low-conductance openings (Fig. 1*A*).

In some PCs (P5–9) we also identified high-conductance single-channel openings with properties typical of NR2A or -2B-containing NMDARs (Cull-Candy *et al.* 2001). These events were detected in PCs from wild-type animals (3 out of 8 patches), where they occurred together with low-conductance openings (and constituted $<$ 10% of openings at −60 mV) (Fig. 1*E*). These events showed an average slope conductance of 53.8 ± 2.9 pS. Consistent with this, similar openings were also detected in 1 of 8 NR2D−/− patches, where the events were readily blocked with extracellular Mg^{2+} (Fig. 1*F*).

High-conductance NMDAR channels are present in PCs from adult mice

Although immunohistochemical methods have identified the presence of NR2A and NR2B subunit protein in PCs of mature mice (Thompson *et al.* 2000), functional NMDARs were thought to be absent. To address this anomaly, we next looked for NMDA-activated whole-cell currents in PCs of adult animals ($\geq$ P50). We found that whole-cell currents

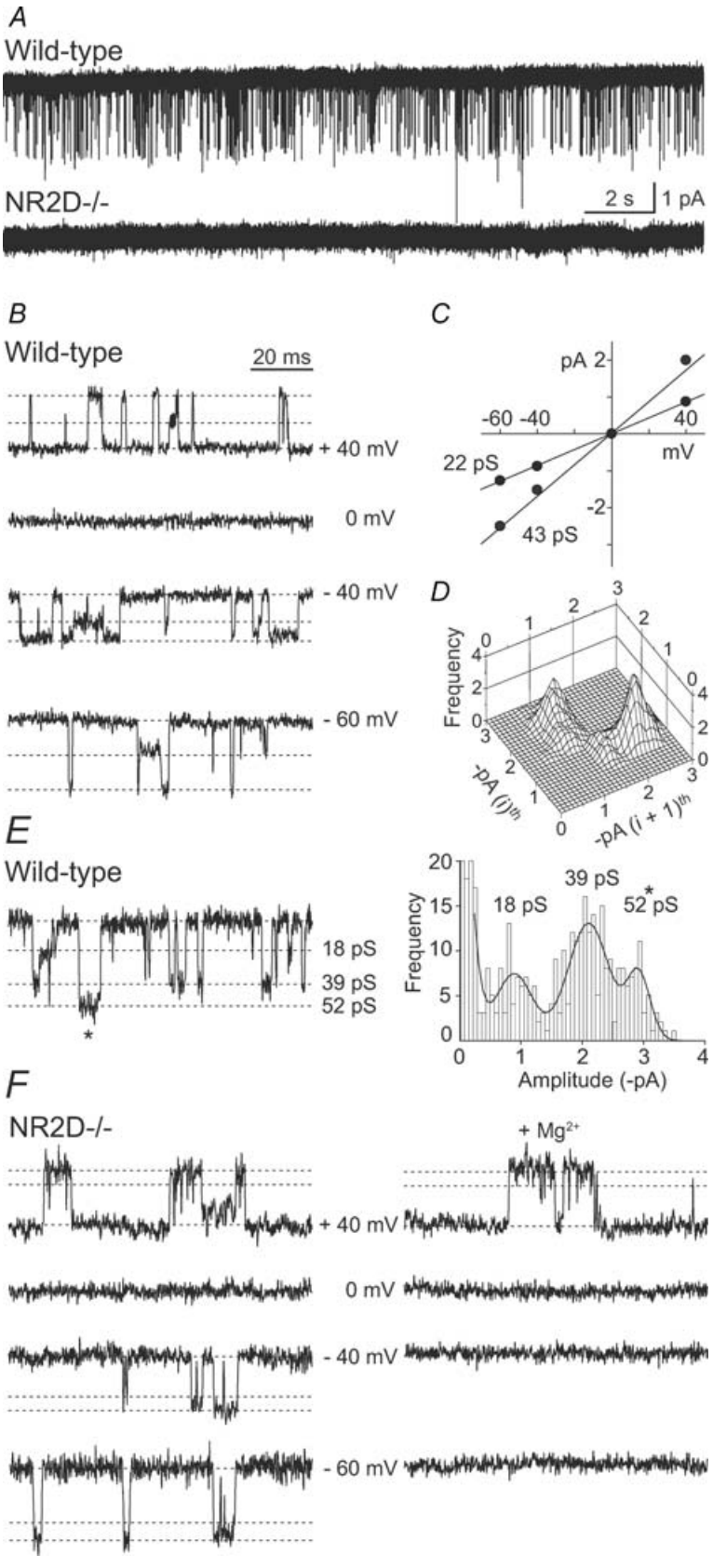

Figure 1. Low- and high-conductance NMDARs in PCs from young mice
A, continuous recording from wild-type and NR2D−/− patches, in the presence of 10 μM NMDA and 5 μM glycine (P6; −60 mV). Single-channel currents are absent from the NR2D−/− patch. *B–D*, properties of NMDARs in wild-type mice. *B*, single-channel currents recorded at various membrane potentials and *C*, the corresponding current–voltage relationship (same patch as *A*). Slope conductances for this patch are indicated on the *I–V* plot, and indicated as dotted lines on the traces. The mean slope conductances from 3 patches were 42.5 ± 1.0 and 21.3 ± 0.3 pS. *D*, typical of NR2D-containing NMDARs, direct transitions from the main- to the subconductance level occurred more frequently than *vice versa*, as shown by the 'asymmetry plot', where i^{th} represents the first and $(i + 1)^{th}$ represents the second subconductance level for each opening (see also Methods). *E* and *F*, high-conductance NMDARs in patches from wild-type and NR2D−/− P6 mice. *E*, example trace, and its all-point histogram, showing both high- and low-conductance openings (wild-type). *F*, NMDAR openings recorded from an NR2D−/− patch (slope conductance 50 and 38 pS) and their block by 2 mM extracellular Mg^{2+} at negative potentials.

were readily induced by bath application of NMDA (13 out of 16 cells) and these were accompanied by a clear increase in current noise (Fig. 2*A*). The mean steady-state current was 222 ± 140 pA with 50 μM NMDA ($n = 3$) and 474 ± 118 pA with 100 μM NMDA ($n = 4$) (with 50 μM added glycine). In all cells, the response to NMDA was readily blocked by 50–100 μM D-AP5 (average inhibition $84 \pm 5\%$ of control, $n = 7$; Fig. 2*A*).

Single-channel currents could also be recorded from excised somatic patches of adult PCs. Using patch pipettes with small tips (10–15 MΩ), we detected NMDAR channel openings in 2 of 6 patches tested with 10 μM NMDA and

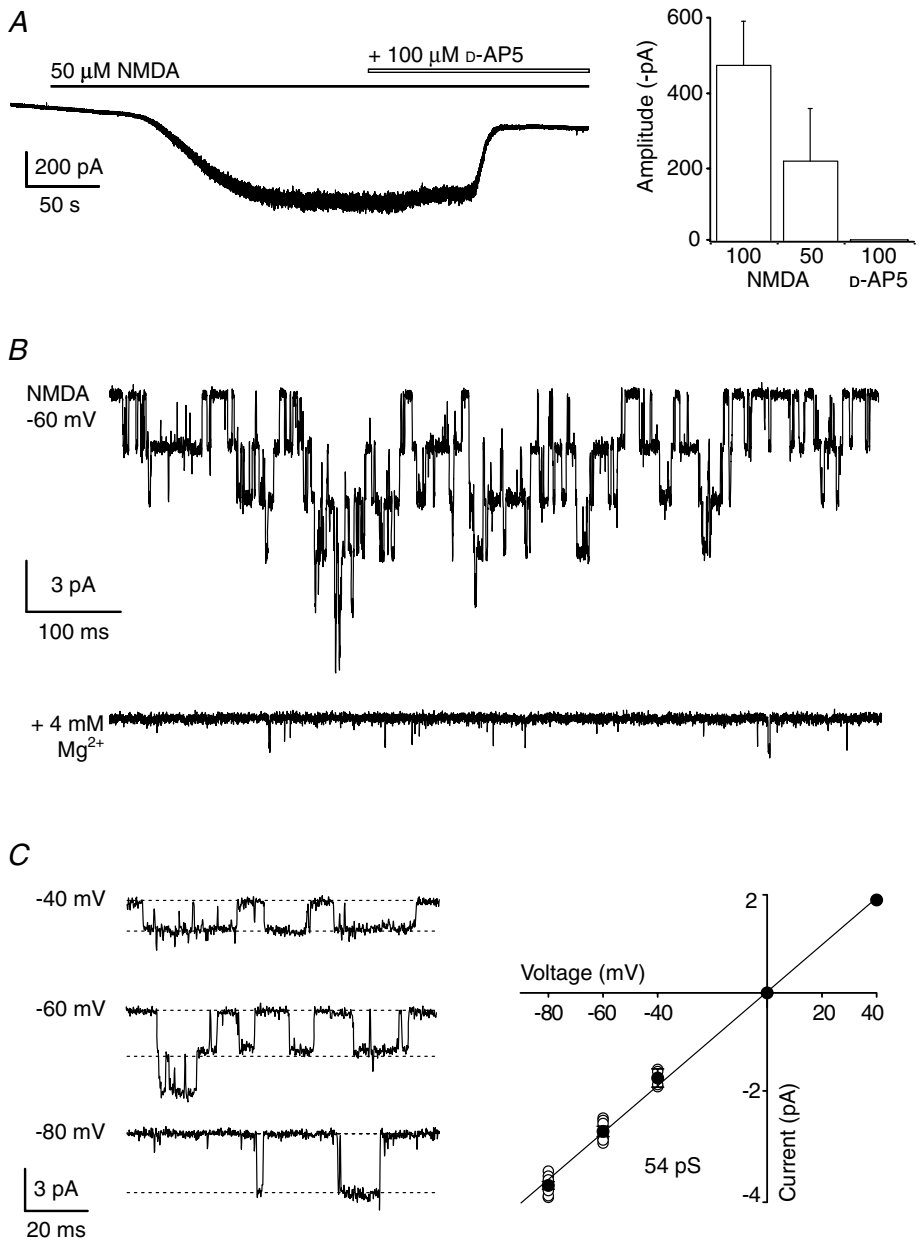

Figure 2. Functional NMDARs in PCs from adult wild-type mice
A, representative whole-cell response to bath applied NMDA (50 μM glycine, −60 mV) and its subsequent block by D-AP5. Right: the bar graph shows amplitudes of currents evoked by different concentrations of NMDA, and block by D-AP5 in pooled data from 7 experiments (concentrations in μM). *B*, superimposed single-channel currents recorded in the presence of 100 μM NMDA (50 μM glycine; −60 mV) in an outside-out patch from a P67 mouse. Lower trace shows block in the presence of Mg^{2+} (4 mM). *C*, NMDA-channel currents recorded at various membrane potentials in a patch from a P74 mouse (100 μM NMDA plus 50 μM glycine; dotted lines indicate the slope conductance for this patch). Right panel shows *I–V* plot of pooled data from 7 experiments (all mice older than P61; mean slope conductance 54 pS).

5 μM glycine. Next, to enable sampling from a greater membrane area, we used larger pipette tips (2–6 MΩ). To further increase the likelihood of observing NMDAR channel openings, we also raised the concentration of applied NMDA (to 50 or 100 μM) and glycine (to 50 μM). The latter would be expected to enhance activation of NR2A-containing NMDARs, which have a low sensitivity to glycine (Kutsuwada *et al.* 1992). In these conditions, single-channel events were detected in 56 of 140 patches (Fig. 2*B* and *C*; slope conductance 53.7 ± 2.2 pS; $n = 7$); as

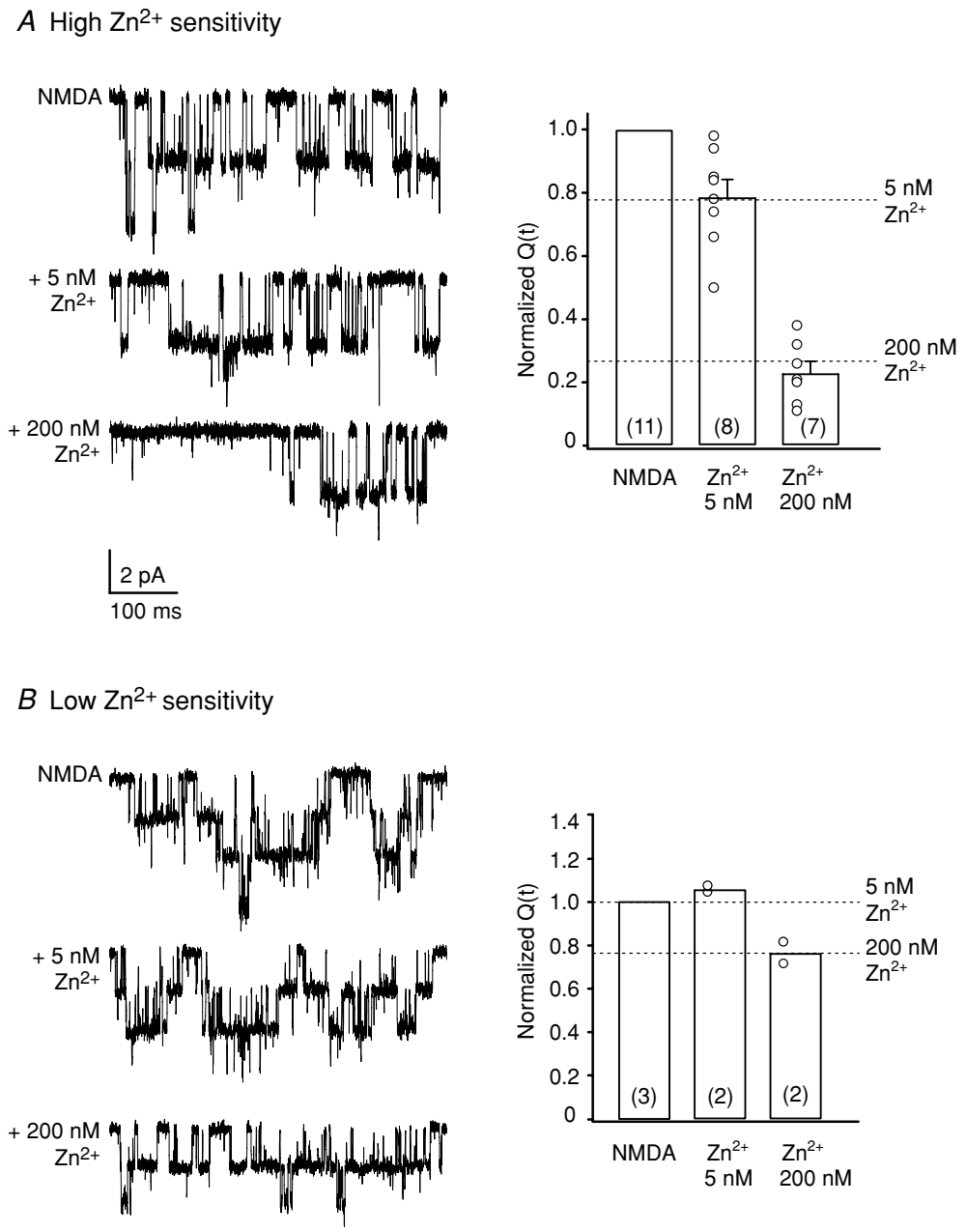

Figure 3. Zinc sensitivity of extrasynaptic NMDARs in PCs from adult mice
A, single-channel currents activated by 100 μM NMDA (50 μM glycine) before and after the application of 5 or 200 nM Zn^{2+} (P74; −60 mV) in an outside-out patch exhibiting 'high' zinc sensitivity. Bar plot shows pooled data from 11 experiments (all mice older than P70) and illustrates the reduction of NMDAR-mediated charge transfer ($Q(t)$) in the presence of Zn^{2+} (symbols indicate values from individual patches; the number of patches is indicated in brackets). Note that, on average, the sensitivity of NMDARs to Zn^{2+} in these patches is typical of recombinant NR2A-containing NMDARs (as indicated by the dotted lines; see Rachline *et al.* 2005). *B*, single-channel currents in a patch exhibiting 'low' zinc sensitivity (P77; −60 mV). Bar plots illustrate pooled data from 3 experiments. Dotted lines indicate the level of Zn^{2+} inhibition expected for recombinant NR2B-containing NMDARs (see Rachline *et al.* 2005).

expected these events were abolished by extracellular Mg^{2+} (2–4 mM) at negative membrane potentials ($n = 10$).

To identify the subunits which gave rise to these NMDAR channel openings, we next tested their sensitivity to nanomolar concentrations of external Zn^{2+}, which is expected to selectively inhibit NR2A-containing NMDARs. In these experiments we used a recording solution buffered with 10 mM tricine (see Methods; Paoletti *et al.* 1997). We found a clear variation between patches in the reduction of NMDAR channel activity induced by 5 and 200 nM Zn^{2+}(Fig. 3), suggesting that receptor types with both high and low sensitivity to Zn^{2+} were present. In the presence of 5 and 200 nM Zn^{2+}, in 11 out of 15 patches, 5 nM Zn^{2+} reduced the charge transfer to $79 \pm 5\%$ of control ($P = 0.0355$; $n = 8$) and 200 nM Zn^{2+} reduced the charge transfer to $23 \pm 4\%$ of control ($P = 0.0015$; $n = 7$) (Fig. 3*A*). The degree of inhibition produced by 200 nM Zn^{2+} was significantly greater than that produced by 5 nM Zn^{2+} ($P < 0.0001$, unpaired Student's *t* test). This degree of inhibition is consistent with the expression of mostly NR1–NR2A receptors (Rachline *et al.* 2005). By contrast, under the same conditions, in 3 out of 15 patches the effects of Zn^{2+} suggested the expression of NR1–NR2B receptors (Rachline *et al.* 2005); 5 nM Zn^{2+} did not affect the charge transfer (~105% of control, $n = 2$), while 200 nM Zn^{2+} reduced the charge transfer to ~77% of control ($n = 2$; Fig. 3*B*). In an additional patch, with multiple openings, the charge transfer was reduced in a manner consistent with the presence of both NR2A- and NR2B-containing NMDARs (data not shown).

We further investigated the presence of NR2B-containing NMDARs in adult PCs by testing the effects of the NR2B subunit-selective blocker ifenprodil (Williams, 1993; Mott *et al.* 1998). In 3 out of 10 patches, 5 μM ifenprodil had no effect on charge transfer ($102.0 \pm 2.6\%$ of control; Fig. 4), suggesting the presence of NR1–NR2A receptors. In the remaining seven patches the blocker produced a modest and variable reduction in charge transfer, to $63.7 \pm 0.5\%$ of control values (range: 89–40%; $P = 0.016$ Wilcoxon matched pairs test). The effect of ifenprodil observed here was clearly less than would be expected for pure NR1–NR2B receptors (~90% inhibition; Hatton & Paoletti, 2005; Fig. 4), suggesting that both NR2B- *and* NR2A-containing NMDARs were expressed in these patches. Taken together with the data on Zn^{2+} sensitivity (Fig. 3), these results suggest that PCs from adult mice express mainly NR2A-containing NMDARs. However, some NR2B-containing NMDARs are present, either in a mixed population of separate NR2A- and NR2B-containing receptors or in tri-heteromeric assemblies (NR1–NR2A–NR2B), or in both.

Activation of NMDARs during CF–PC EPSCs

We next considered whether synaptic release of glutamate, associated with CF-EPSCs, could activate NMDARs

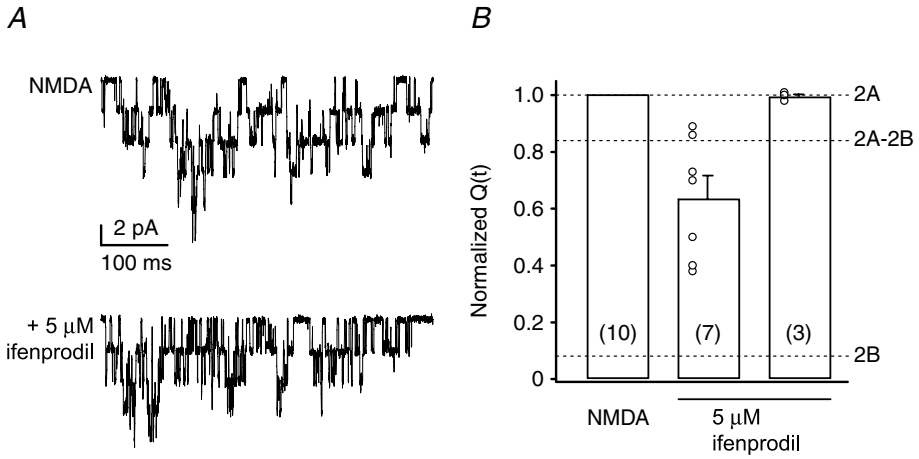

Figure 4. Ifenprodil sensitivity of extrasynaptic NMDARs in PCs from adult mice
A, superimposed NMDAR channel openings in an outside-out patch from an adult PC exposed to 100 μM NMDA (50 μM glycine) before and after the application of 5 μM ifenprodil (P63; −60 mV). In this patch, ifenprodil reduced channel activity. *B*, bar plot of pooled data from 10 experiments showing that, on average, ifenprodil reduced the NMDAR charge transfer ($Q(t)$) to $63.7 \pm 0.5\%$ of control. Note that some patches (right hand bar) were unaffected by ifenprodil. Symbols indicate values from individual patches. Note that the scatter of the data was likely to be due to the presence of more than one NMDAR in each patch. Dotted lines indicate the level of inhibition expected for recombinant NR2A-, NR2A–NR2B- or NR2B-containing NMDAR, in the presence of 3 μM ifenprodil (see Hatton & Paoletti, 2005).

in adult PCs (P62–76). CF stimulation evoked large AMPAR-mediated EPSCs that exhibited characteristic all-or-none activation and paired-pulse depression. In order to allow a reasonable fidelity of voltage-clamp, we recorded CF-EPSCs in the presence of a low concentration of the AMPAR antagonist NBQX (1 μM). The EPSC peak current under these conditions was 397 ± 50 pA ($n = 11$). Following application of an additional 20 μM NBQX, when most AMPARs would be expected to be blocked, residual currents were seen in 7 of 15 cells (97 ± 23 pA). Following addition of 50–100 μM D-AP5, the CF-EPSC peak current was reduced by $76 \pm 5\%$ ($P = 0.0134$) and the charge transfer associated with this residual current was reduced by $80 \pm 6\%$ ($P = 0.0083$) (Fig. 5). The D-AP5-sensitive component of the EPSCs exhibited paired-pulse depression characteristic of CF responses, but rose significantly more slowly than the NBQX-sensitive (AMPAR-mediated) component of CF-EPSCs (10–90% rise time 8.8 ± 1.1 ms *versus* 3.0 ± 0.5 ms; $P = 0.0003$; $n = 7$; Fig. 5*A*). These data indicate that CF stimulation can activate NMDARs in adult PCs.

To investigate the NMDAR subtypes underlying CF-EPSCs, we examined their sensitivity to 5 μM ifenprodil. Neither the peak current nor the charge transfer (recorded in the presence of 20 μM NBQX) was affected.

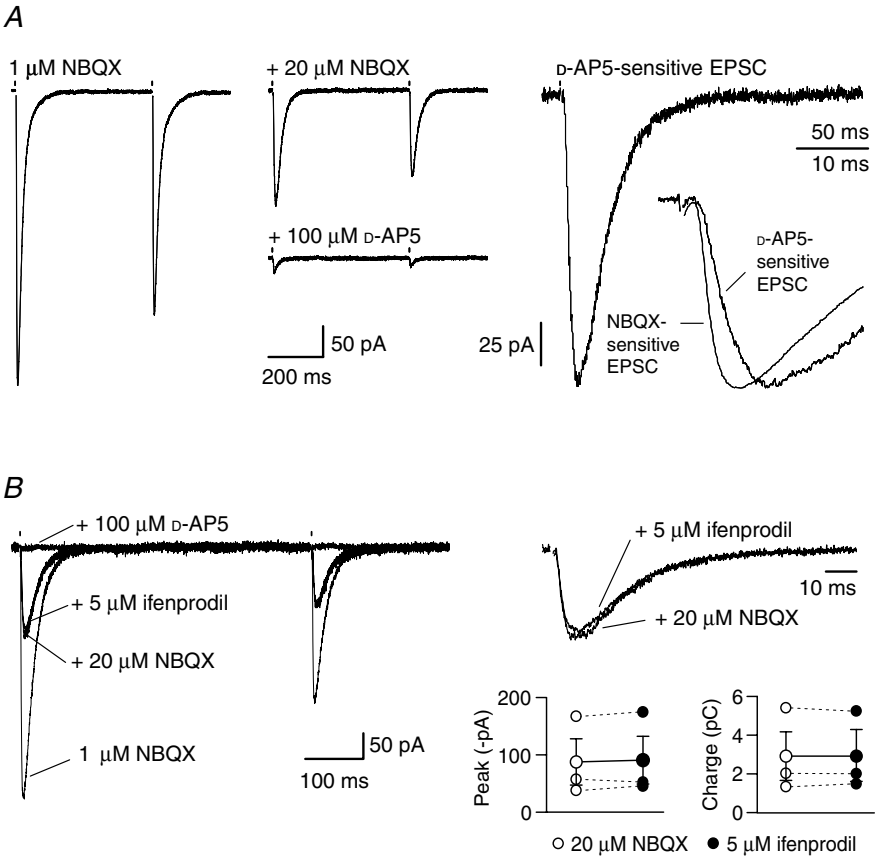

Figure 5. NMDAR activation during CF-EPSC in PCs from adult mice
A, CF-EPSCs evoked in 1 μM NBQX (left). After full block of remaining AMPARs by an additional 20 μM NBQX (middle), CF-EPSCs were greatly reduced by D-AP5. The D-AP5-sensitive current is shown on the right. As illustrated in the inset (scaled currents), this NMDAR-mediated component rose more slowly than the pure AMPAR-mediated component of the EPSC (NBQX-sensitive current). In this cell the 10–90% rise time was 6.2 ms (*versus* 2.4 ms for the NBQX-sensitive current) and the 37% decay was 27 ms; mean 37% decay 29 ± 4 ms ($n = 7$). The D-AP5-sensitive current was obtained by subtracting the average CF-EPSC recorded in the presence of 50–100 μM D-AP5 from the average CF-EPSC recorded in the presence of 20 μM NBQX. The NBQX-sensitive current was obtained by subtracting the average CF-EPSC recorded in the presence of 20 μM NBQX from the average CF-EPSC recorded in the presence of 1 μM NBQX. *B*, CF-EPSCs from a different PC, recorded initially in the presence of 1 μM NBQX. Addition of a further 20 μM NBQX left a residual component that was unaffected by 5 μM ifenprodil but eliminated by D-AP5. Right: same traces on an expanded time scale. Stimulation artefacts were blanked. Bottom right: plot of pooled data from 3 experiments showing the lack of effect of ifenprodil on the peak and the area (charge) of NMDAR-mediated CF-EPSCs (see text for details). Symbols connected by continuous lines show the mean values and the vertical error bars indicate the S.E.M.

The peak current was 86 ± 40 pA in NBQX and 89 ± 42 pA in ifenprodil ($P = 0.465$). The charge transfer was also unchanged (3.1 ± 1.2 pC *versus* 3.1 ± 1.3 pC, $P = 0.934$; $n = 3$; Fig. 5*B*). These data are consistent with the view that CF stimulation activates mainly NR2A-containing NMDARs in adult PCs.

Discussion

Our experiments demonstrate the following. First, low-conductance NMDAR channels are present in PCs from young mice, but absent from NR2D−/− animals, confirming that they arise from NR2D-containing NMDARs, as previously proposed (Momiyama *et al.* 1996). Second, distinct high-conductance NMDAR subtypes are also expressed in PCs of young mice, whilst *only* high-conductance (NR2A- or NR2B-containing) NMDAR subtypes are present in PCs of adult mice. Third, NMDARs can be activated during the CF-evoked EPSC.

Previous investigations have addressed the question of whether NMDARs are present in PCs. Here, using NR2D−/− mice, we confirmed the key role of NR2D subunits in the formation of NMDARs in PCs of young animals (Momiyama *et al.* 1996). Furthermore, we have identified high-conductance (NR2A- or NR2B-containing) NMDARs in PCs from these NR2D−/− mice, confirming that receptors formed from other subunits can also be expressed, albeit with a low frequency of occurrence. Such receptors were also evident in wild-type PCs (see also Rosenmund *et al.* 1992). Perhaps more surprisingly, our experiments clearly indicate that PCs from *adult* mice also express functional high-conductance NMDARs. The sensitivity of these receptors to Zn^{2+} ions suggests that while most NMDAR assemblies contain the NR2A subunit, some NR2B-containing receptors are also present (Rachline *et al.* 2005). This interpretation is supported by our results with the NR2B-selective antagonist ifenprodil.

While most patches exhibited some sensitivity to ifenprodil (5 μM), the degree of inhibition varied widely and was always incomplete (Fig. 4). At this concentration, ifenprodil produces almost complete block of recombinant NR1–NR2B receptors (Hatton & Paoletti, 2005), while in our adult PC patches it reduced NMDAR-channel activity by only ∼40%. These results suggest that while NR2B subunits are expressed, they are present in only a minority of extrasynaptic NMDARs. Overall, our data indicate that extrasynaptic NMDARs in adult PCs are predominantly NR1–NR2A assemblies, with some NR2B-containing receptors also expressed, either as NR1–NR2B assemblies or as tri-heteromeric NR1–NR2A–NR2B receptors (Vicini *et al.* 1998). Native high-conductance tri-heteromeric NR1–NR2B–NR2D receptors have been reported elsewhere (Brickley *et al.* 2003) and such receptors could be present in PCs of both young and adult mice. Although a lack of consensus in the data from *in situ* hybridization (Watanabe *et al.* 1994) and immunolabelling (Thompson *et al.* 2000) does not allow us to exclude this possibility in the adult, it seems unlikely given the absence of low-conductance (NR2D-containing) NMDARs from mature PCs (Momiyama *et al.* 1996; present study).

Importantly, we show that NMDARs can be activated during CF-EPSCs in adult PCs, as demonstrated by the presence of a small but significant D-AP5-sensitive component of CF-evoked current. This component was unaffected by ifenprodil, suggesting the EPSC was mediated by NR2A-containing NMDARs, as described at a number of adult synapses (Stocca & Vicini, 1998; Quinlan *et al.* 1999; Townsend *et al.* 2003; van Zundert *et al.* 2004).

Consistent with this interpretation, the decay of the NMDAR-mediated current was relatively rapid in the adult PCs (37% decay ∼29 ms; Fig. 5), and comparable to that of recombinant NR2A-containing NMDARs (Vicini *et al.* 1998). Rapidly decaying synaptic currents (weighted decay ∼33 ms) have also been described in hippocampal neurons cultured from NR2B−/− mice (Tovar *et al.* 2000), and have similarly been attributed to NR2A-containing NMDARs. The residual CF-EPSC recorded in the presence of high concentrations of both NBQX and D-AP5 could be due to the presence of GluR5 kainate receptors, although the magnitude of this current was much smaller than that reported in younger mice (Huang *et al.* 2004). Finally, the absence of a glutamate transporter current in our conditions reflects the presence of Cl^- as the major anion in the pipette solution (Otis *et al.* 1997).

In principle, NMDARs at the CF–PC synapse could mediate a small phasic influx of Ca^{2+} with a spatiotemporal profile potentially different from that of Ca^{2+} elevation associated with CF-evoked complex spikes (Hartmann & Konnerth, 2005). The absence of an NMDAR-mediated CF-EPSC in PCs from juvenile or adult rats (Perkel *et al.* 1990; Llano *et al.* 1991; Otis *et al.* 1997; Auger & Attwell, 2000) may reflect a species difference. It is of note that PCs from adult human tissue show labelling for NR1, NR2A and NR2D mRNA (Scherzer *et al.* 1997) and are therefore also likely to express functional NMDARs. These could participate in synaptic transmission and pathological conditions likely to involve excitotoxicity (Slemmer *et al.* 2005).

References

Auger C & Attwell D (2000). Fast removal of synaptic glutamate by postsynaptic transporters. *Neuron* **28**, 547–558.

Brickley SG, Misra C, Mok MH, Mishina M & Cull-Candy SG (2003). NR2B and NR2D subunits coassemble in cerebellar Golgi cells to form a distinct NMDA receptor subtype restricted to extrasynaptic sites. *J Neurosci* **23**, 4958–4966.

Cull-Candy S, Brickley S & Farrant M (2001). NMDA receptor subunits: diversity, development and disease. *Curr Opin Neurobiol* **11**, 327–335.

Dingledine R, Borges K, Bowie D & Traynelis SF (1999). The glutamate receptor ion channels. *Pharmacol Rev* **51**, 7–61.

Dzubay JA & Otis TS (2002). Climbing fiber activation of metabotropic glutamate receptors on cerebellar Purkinje neurons. *Neuron* **36**, 1159–1167.

Farrant M & Cull-Candy SG (1991). Excitatory amino acid receptor-channels in Purkinje cells in thin cerebellar slices. *Proc R Soc Lond B Biol Sci* **244**, 179–184.

Furukawa H, Singh SK, Mancusso R & Gouaux E (2005). Subunit arrangement and function in NMDA receptors. *Nature* **438**, 185–192.

Hartmann J & Konnerth A (2005). Determinants of postsynaptic Ca^{2+} signaling in Purkinje neurons. *Cell Calcium* **37**, 459–466.

Hatton CJ & Paoletti P (2005). Modulation of triheteromeric NMDA receptors by N-terminal domain ligands. *Neuron* **46**, 261–274.

Huang YH, Dykes-Hoberg M, Tanaka K, Rothstein JD & Bergles DE (2004). Climbing fiber activation of EAAT4 transporters and kainate receptors in cerebellar Purkinje cells. *J Neurosci* **24**, 103–111.

Ikeda K, Araki K, Takayama C, Inoue Y, Yagi T, Aizawa S & Mishina M (1995). Reduced spontaneous activity of mice defective in the $\epsilon 4$ subunit of the NMDA receptor channel. *Brain Res Mol Brain Res* **33**, 61–71.

Kakegawa W, Tsuzuki K, Iino M & Ozawa S (2003). Functional NMDA receptor channels generated by NMDAR2B gene transfer in rat cerebellar Purkinje cells. *Eur J Neurosci* **17**, 887–891.

Kutsuwada T, Kashiwabuchi N, Mori H, Sakimura K, Kushiya E, Araki K, Meguro H, Masaki H, Kumanishi T, Arakawa M & Mishina M (1992). Molecular diversity of the NMDA receptor channel. *Nature* **358**, 36–41.

Llano I, Marty A, Armstrong CM & Konnerth A (1991). Synaptic- and agonist-induced excitatory currents of Purkinje cells in rat cerebellar slices. *J Physiol* **434**, 183–213.

Momiyama A, Feldmeyer D & Cull-Candy SG (1996). Identification of a native low-conductance NMDA channel with reduced sensitivity to Mg^{2+} in rat central neurones. *J Physiol* **494**, 479–492.

Momiyama A, Silver RA, Hausser M, Notomi T, Wu Y, Shigemoto R & Cull-Candy SG (2003). The density of AMPA receptors activated by a transmitter quantum at the climbing fibre-Purkinje cell synapse in immature rats. *J Physiol* **549**, 75–92.

Mott DD, Doherty JJ, Zhang S, Washburn MS, Fendley MJ, Lyuboslavsky P, Traynelis SF & Dingledine R (1998). Phenylethanolamines inhibit NMDA receptors by enhancing proton inhibition. *Nat Neurosci* **1**, 659–667.

Neyton J & Paoletti P (2006). Relating NMDA receptor function to receptor subunit composition: limitations of the pharmacological approach. *J Neurosci* **26**, 1331–1333.

Otis TS, Kavanaugh MP & Jahr CE (1997). Postsynaptic glutamate transport at the climbing fiber-Purkinje cell synapse. *Science* **277**, 1515–1518.

Paoletti P, Ascher P & Neyton J (1997). High-affinity zinc inhibition of NMDA NR1-NR2A receptors. *J Neurosci* **17**, 5711–5725.

Perkel DJ, Hestrin S, Sah P & Nicoll RA (1990). Excitatory synaptic currents in Purkinje cells. *Proc Biol Sci* **241**, 116–121.

Petralia RS, Yokotani N & Wenthold RJ (1994). Light and electron microscope distribution of the NMDA receptor subunit NMDAR1 in the rat nervous system using a selective anti-peptide antibody. *J Neurosci* **14**, 667–696.

Quinlan EM, Philpot BD, Huganir RL & Bear MF (1999). Rapid, experience-dependent expression of synaptic NMDA receptors in visual cortex in vivo. *Nat Neurosci* **2**, 352–357.

Rachline J, Perin-Dureau F, Le Goff A, Neyton J & Paoletti P (2005). The micromolar zinc-binding domain on the NMDA receptor subunit NR2B. *J Neurosci* **25**, 308–317.

Rosenmund C, Legendre P & Westbrook GL (1992). Expression of NMDA channels on cerebellar Purkinje cells acutely dissociated from newborn rats. *J Neurophysiol* **68**, 1901–1905.

Scherzer CR, Landwehrmeyer GB, Kerner JA, Standaert DG, Hollingsworth ZR, Daggett LP, Veliçelebi G, Penney JB Jr & Young AB (1997). Cellular distribution of NMDA glutamate receptor subunit mRNAs in the human cerebellum. *Neurobiol Dis* **4**, 35–46.

Slemmer JE, De Zeeuw CI & Weber JT (2005). Don't get too excited: mechanisms of glutamate-mediated Purkinje cell death. *Prog Brain Res* **148**, 367–390.

Stocca G & Vicini S (1998). Increased contribution of NR2A subunit to synaptic NMDA receptors in developing rat cortical neurons. *J Physiol* **15**, 13–24.

Thompson CL, Drewery DL, Atkins HD, Stephenson FA & Chazot PL (2000). Immunohistochemical localization of *N*-methyl-D-aspartate receptor NR1, NR2A, NR2B and NR2C/D subunits in the adult mammalian cerebellum. *Neurosci Lett* **283**, 85–88.

Tovar KR, Sprouffske K & Westbrook GL (2000). Fast NMDA receptor-mediated synaptic currents in neurons from mice lacking the $\epsilon 2$ (NR2B) subunit. *J Neurophysiol* **83**, 616–620.

Townsend M, Yoshii A, Mishina M & Constantine-Paton M (2003). Developmental loss of miniature N-methyl-D-aspartate receptor currents in NR2A knockout mice. *Proc Natl Acad Sci U S A* **100**, 1340–1345.

van Zundert B, Yoshii A & Constantine-Paton M (2004). Receptor compartmentalization and trafficking at glutamate synapses: a developmental proposal. *Trends Neurosci* **27**, 428–437.

Vicini S, Wang JF, Li JH, Zhu WJ, Wang YH, Luo JH, Wolfe BB & Grayson DR (1998). Functional and pharmacological differences between recombinant N-methyl-D-aspartate receptors. *J Neurophysiol* **79**, 555–566.

Watanabe M, Mishina M & Inoue Y (1994). Distinct spatiotemporal expressions of five NMDA receptor channel subunit mRNAs in the cerebellum. *J Comp Neurol* **343**, 513–519.

Williams K (1993). Ifenprodil discriminates subtypes of the N-methyl-D-aspartate receptor: selectivity and mechanisms at recombinant heteromeric receptors. *Mol Pharmacol* **44**, 851–859.

Wyllie DJ, Behe P, Nassar M, Schoepfer R & Colquhoun D (1996). Single-channel currents from recombinant NMDA NR1a/NR2D receptors expressed in *Xenopus* oocytes. *Proc Biol Sci* **263**, 1079–1086.

Acknowledgements

This work was supported by a Wellcome Trust Programme Grant (SGC-C and MF) and the Institute Pasteur-Fondazione Cenci Bolognetti (MR). S.G.C.-C. holds a Royal Society-Wolfson Award. We thank Masayoshi Mishina, University of Tokyo, for generous help in providing NR2D−/− mice.